



Cite this: *CrystEngComm*, 2015, 17, 3297

Mother structures related to the hexagonal and cubic close packing in Cu₂₄ clusters: solvent-influenced derivatives†

Eder Amayuelas,^a Arkaitz Fidalgo-Marijuan,^a Gotzone Barandika,^{*b} Begoña Bazán,^{ac} Miren-Karmele Urriaga^a and María Isabel Arriortua^{ac}

Compound **1** [Cu₂₄(*m*-BDC)₂₄(DMF)₂₀(H₂O)₄]·24DMF·40H₂O (*m*-BDC is 1,3-benzenedicarboxylate and DMF is *N,N*-dimethylformamide) has been synthesized and structurally characterized by X-ray diffraction. It consists of Cu₂₄ clusters arranged in such a way that 12 dimers are connected through *m*-BDC ligands. The clusters exhibit an internal cavity where crystallization molecules of DMF and water are located. Additionally, there are guest DMF and water molecules in the voids generated by the 3D packing of the Cu₂₄ clusters. The thermal stability of compound **1** has also been characterized, concluding that hydrogen bonds between solvent molecules are responsible for the robustness of the network. Compound **1** is similar to seven other compounds found in the literature. This work is focused on the crystallochemical comparison of these compounds, which concludes that there are two mother structures related to the hexagonal and cubic close packing of polyhedra. Derivative compounds are produced in the presence of different solvent molecules (differences affecting both the nature and the number of the guest molecules).

Received 3rd February 2015,
Accepted 19th March 2015

DOI: 10.1039/c5ce00251f

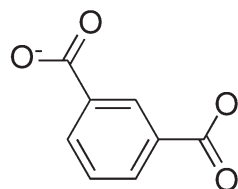
www.rsc.org/crystengcomm

Introduction

In supramolecular coordination architectures, metal–organic M₂₄ clusters (M = transition metal) have attracted particular interest due to their well-defined and confined cavities, high symmetry and stability, and rich chemical and physical properties and functions.^{1–5} In the past decade, great advances have been done in the design, synthesis and characterization of these compounds, despite the difficulties they entail, for instance, the high requirements in crystallographic accuracy. Furthermore, crystal growth is especially relevant in this type of compound since the principle of maximum space filling in crystal structures often produces outstanding phenomena like interpenetrated frameworks.^{6–9} Therefore, the role of void-filling solvents is rather significant as different frameworks can be produced in dissolution-started crystallization processes. In fact, in these cases, solvents provide van der Waals forces driving the crystal growth, where those small molecules

are strategically packed to stabilize the network. Solvent molecules can also complete coordination polyhedra around metal ions in SCFs (solid coordination frameworks). On the other hand, crystal growth has a direct influence on the morphology of the crystals.¹⁰ Obviously, aspects related to the role of solvents are especially remarkable in porous compounds since, in many cases, the cavities contain solvent molecules.

This work is focused on a new SCF. This type of compound has been extensively studied during the past decade due to the variety of structures that can be formed by using metal complexes as synthons.^{11–15} In fact, this work reports [Cu₂₄(*m*-BDC)₂₄(DMF)₂₀(H₂O)₄]·24DMF·40H₂O (**1**), where *m*-BDC is 1,3-benzenedicarboxylate (Scheme 1) and DMF is *N,N*-dimethylformamide, since the features exhibited by this compound give us the opportunity of discussing most of the above-mentioned aspects. Thus, compound **1** consists of Cu₂₄ clusters arranged in such a way that 12 dimers are connected through *m*-BDC ligands.



1,3-benzenedicarboxylate

Scheme 1 Lewis structure of 1,3-benzenedicarboxylate (*m*-BDC).

^a Departamento de Mineralogía y Petrología, Universidad del País Vasco (UPV/EHU), Barrio Sarriena s/n, 48940 Leioa, Bizkaia, Spain

^b Departamento de Química Inorgánica, Universidad del País Vasco (UPV/EHU), Barrio Sarriena s/n, 48940 Leioa, Bizkaia, Spain. E-mail: gotzone.barandika@ehu.es

^c BC Materials, Basque Center for Materials, Applications and Nanostructures, Parque Tecnológico de Zamudio, Ibaizabal Bidea, Edificio 500-Planta 1, 48160 Derio, Bizkaia, Spain

† Electronic supplementary information (ESI) available: ORTEP detail of the structure, IR spectra, thermogravimetry, and X-ray thermodiffraction and crystallographic data. CCDC 1034874. For ESI and crystallographic data in CIF or other electronic format see DOI: 10.1039/c5ce00251f

The interest in compound **1** lies on the fact that seven similar clusters have been reported so far.^{16–18} However, a comparison of the eight compounds (including compound **1**) reveals the variety in the 3D packing fashions produced by similar, discrete, large clusters. This comparison also permits discussion on the role of solvents acting as crystallization molecules and their influence on the packing modes. Furthermore, this work provides some examples of the risk associated with visualization of crystal structures, especially when figures intend to transmit the existence of large cavities by omitting the presence of crystallization molecules.

Another point for discussion is the risk associated with the interpretation of raw crystallographic data. Thus, while structural parameters for the eight compounds to be compared are quite different, a deep analysis reveals that they form two families: related to the hexagonal and cubic close packing of spheres (HCP and CCP, respectively, Scheme 2). Finally, as compound **1** has been synthesized through two distinct routes, this work also presents an example of the role of crystallization helpers in obtaining crystals with different sizes.¹⁹

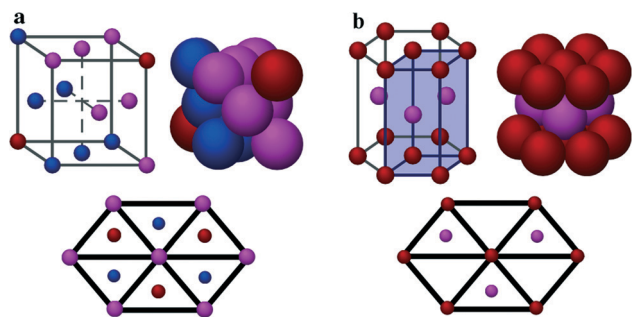
Experimental section

General

All solvents and chemicals were used as received from reliable commercial sources. The reagents protoporphyrin IX, 1,3-isophthalic acid, and copper(II) nitrate hydrate (99%) and the solvent *N,N*-dimethylformamide (DMF, 99.8%) were purchased from Sigma-Aldrich Co.

Synthesis of $[\text{Cu}_{24}(\text{m-BDC})_{24}(\text{DMF})_{20}(\text{H}_2\text{O})_4] \cdot 24\text{DMF} \cdot 40\text{H}_2\text{O}$

$\text{Cu}(\text{NO}_3)_2 \cdot x\text{H}_2\text{O}$ (12.9 mg, 0.06 mmol) and 1,3-isophthalic acid (*m*-BDC) (9.9 mg, 0.06 mmol) were added to DMF (4.5 mL) in a small capped vial and heated to 100 °C for 72 h, yielding diffraction quality prismatic turquoise crystals. By adding protoporphyrin IX (5.9 mg, 0.01 mmol) to the above-mentioned procedure, higher quality and bigger crystals were obtained (found: C, 38.13(4); H, 3.78(5); N, 2.38(3); O, 32.65(3). Calc. for $\text{C}_{237}\text{H}_{232}\text{Cu}_{24}\text{N}_{16}\text{O}_{133}$: C, 40.92; H, 3.36; N, 3.22; O, 30.58).



Scheme 2 (a) Cell for cubic close packing. (b) Cell for hexagonal close packing.

Single-crystal X-ray diffraction

Prismatic turquoise single crystals of compound **1** with dimensions given in Table 1 were selected under a polarizing microscope and mounted on MicroMounts™. Single-crystal X-ray diffraction data were collected at 100 K using a SuperNova single source diffractometer with Cu $K\alpha$ radiation ($\lambda = 1.54184$ Å). Data frames were processed (unit cell determination, intensity data integration, correction for Lorentz and polarization effects,²⁰ and analytical absorption correction) using the CrysAlisPro software package.²¹

The structure of **1** was solved in the triclinic $P\bar{1}$ space group with the Superflip program,²² which allowed us to obtain the position of Cu atoms, as well as some of the oxygen, nitrogen and carbon atoms of the isophthalic acid and DMF molecules. The initial refinement of the crystal structure was performed by conjugate-gradient least-squares using the CGLS instruction in the SHELXL-97 program,²³ since the final cycles were performed by full matrix least-squares based on F^2 , using the SHELXL-97 program²³ in OLEX²⁴ obtaining the remaining nitrogen, oxygen and carbon atoms. Anisotropic thermal parameters were used for all nonhydrogen atoms involved in the cuboctahedron, as well as for DMF molecules fully occupying the crystallographic positions. The water and DMF solvent molecules partially occupying the crystallographic positions as well as the

Table 1 Crystallographic data for **1**

Compound	$[\text{Cu}_{24}(\text{m-BDC})_{24}(\text{DMF})_{20}(\text{H}_2\text{O})_4] \cdot 24\text{DMF} \cdot 40\text{H}_2\text{O}$
Formula	$\text{C}_{297.58}\text{H}_{466}\text{Cu}_{24}\text{N}_{35.6}\text{O}_{172.7}$
FW, g mol ⁻¹	8830.49
Crystal system	Triclinic
Space group (no. 2)	$P\bar{1}$
<i>a</i> , Å	24.4797(3)
<i>b</i> , Å	24.5938(3)
<i>c</i> , Å	25.2374(3)
α , deg	118.4357(13)
β , deg	111.9694(11)
γ , deg	94.2287(10)
<i>V</i> , Å ³	11 784.9 (2)
<i>Z</i>	1
$\rho_{\text{obs}}, \rho_{\text{calc}}$, g cm ⁻³	1.346(5), 1.072
<i>F</i> (000)	3784
μ , mm ⁻¹	1.737
Crystal size, mm	0.27 × 0.21 × 0.08
Absorption correction	Analytical
Radiation, λ , Å	1.54184
Temperature, K	100(2)
Reflections collected, unique	155 317, 41 318 ($R_{\text{int}} = 0.04$)
Limiting indices	$-29 \leq h \leq 29$ $-27 \leq k \leq 28$ $-30 \leq l \leq 28$
Refinement method	Conjugate-gradient and full-matrix least-squares on F^2
Final <i>R</i> indices [$I > 2\sigma(I)$] ^a	$R_1 = 0.0859$, $wR_2 = 0.2564$
<i>R</i> indices (all data) ^a	$R_1 = 0.0975$, $wR_2 = 0.2744$
Goodness of fit on F^2	1.087
Parameters/restraints	2154/47

$$^a R_1 = [(|F_o| - |F_c|)/|F_o|], wR_2 = [w(|F_o|^2 - |F_c|^2)^2]/[w(|F_o|^2)^2]^{1/2}.$$

hydrogen atoms were refined isotropically (Fig. S1, ESI†). The hydrogen atoms of the DMF and water molecules were not considered due to the lack of density in the residual density map; however, they are included in the formula. Although 36 DMF and 24 water molecule positions were localized during the crystal structure refinement process, many of the solvent molecules were disordered in the crystal and the resulting electron density was found to be non-interpretable (density corresponding to 520 e⁻ was removed per unit cell). Taking into account the single crystal experimental density²⁵ (1.346(5) g cm⁻³), the removed electrons and the calculated free effective volume (explained below), our estimation is that 8 DMF and 20 water molecules per formula unit have been ignored during the structure refinement process, although they were included in the chemical formula. The solvent contribution to the structure factors was taken into account by back-Fourier transformation of all densities found in the disordered area using the SQUEEZE program in PLATON.²⁶ The diffraction data were able to show DMF solvent molecules in 16 different positions giving a total occupancy of 12 molecules. In the case of water molecules, 20 H₂O molecules were disordered in 23 different positions. A total of 20 coordination DMF molecules gives a total occupancy of 16, since two of the four coordination water positions were fully occupied and the other two were disordered in four positions with 50% each.

The position of some carbon, nitrogen and oxygen atoms in the DMF molecules was fixed using DFIX and DANG instructions in the refinement to adjust the C–N distance to 1.45 or 1.33 Å, the C=O distance to 1.23 Å and the C–N–C angle to 120°. Bond distances and angles, atomic coordinates, anisotropic thermal parameters and hydrogen atom coordinates are given in Tables S2–S4 (ESI†).

From a crystallographic point of view, compound **1** can be described by using $Z = 2$, in accordance with the space group and the asymmetric unit. However, $Z' = 1$ has been considered because this way the whole cuboctahedron is represented in the chemical formula.

Physicochemical characterization techniques

The IR spectra were collected using a JASCO FT/IR-6100 spectrometer at room temperature in the range of 4000–400 cm⁻¹, in KBr pellets (1% of the sample). C, H, N and O elemental analyses were measured using a Euro EA 3000 elemental analyzer. Thermogravimetric analyses were carried out using a NETZSCH STA 449F3 thermobalance. A crucible containing approximately 10 mg of sample was heated at 5 °C min⁻¹ in the temperature range of 30–600 °C. The thermal behaviour was also studied by using X-ray thermogravimetry. A Bruker D8 Advance Vantec diffractometer (Cu–K α radiation) equipped with a variable-temperature stage (Anton Paar HTK2000) with a Pt sample holder was used in the experiments. The powder patterns were recorded in 2 θ steps of 0.0333° in the 5–38° range, counting for 0.8 s per

step and increasing the temperature at 15 °C min⁻¹ from room temperature to 600 °C.

Results and discussion

Crystal growth

As commonly experienced by researchers, sometimes the result of a synthetic route is not the desired one, and this is exactly what happened in the synthesis of compound **1**. In fact, we intended to produce metalloporphyrin-based SCFs,^{27–30} but instead the synthesis yielded large, good-quality crystals of **1**. Then, we confirmed that the presence of protoporphyrin IX was not necessary to synthesize compound **1**. However, synthesis of **1** without protoporphyrin IX results in smaller, lower-quality, single crystals. Therefore, protoporphyrin IX acts as a crystallization helper. Fig. 1 shows the aspect of the single crystals obtained with and without the crystallization helper. As observed, in both cases single crystals exhibit a prismatic habit. However, the use of the helper results in crystals up to ten times larger.

Crystal structure

Compound **1** consists of Cu₂₄ clusters arranged in such a way that 12 dimers are connected through *m*-BDC ligands (Fig. 2). The *m*-BDC ligands are also responsible for the connections between the Cu^{II} ions forming the dimers. The clusters exhibit an internal cavity where crystallization molecules of DMF and water are located. Additionally, there are guest DMF and water molecules located in the voids generated by the 3D packing of the Cu₂₄ clusters (this point will be discussed below).

The space group is $P\bar{1}$ implying that there is an inversion centre. As observed in Fig. 2, the Cu₂₄ clusters are cuboctahedric units, and the twelve dimers consist of two Cu^{II} square pyramids (SP). The disposition of the twelve dimers is analogous to the cubic close packing of spheres (CCP), but in this case the central position is occupied by a crystallization molecule of water (located at an inversion centre).

Each SP has four oxygen atoms belonging to four different *m*-BDC ligands. Both SPs in each dimer are linked through Cu–O–C–O–Cu bridges, so they have their bases opposite to each other. The apical positions are occupied by DMF and

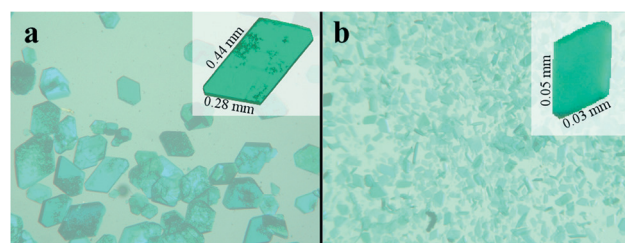


Fig. 1 Single crystals of compound **1** using protoporphyrin IX as a crystallization helper (a) and without it (b).

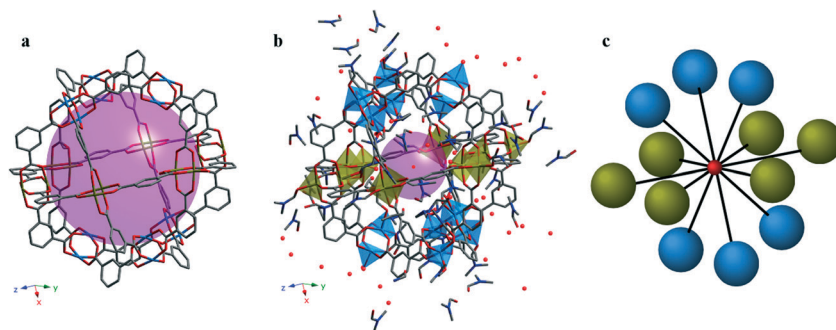


Fig. 2 View of the Cu_{24} cluster (a) where solvent molecules have been omitted and (b) where localized solvent molecules per formula unit are shown. The purple spheres represent the accessible volume: $a = 2145 \text{ \AA}^3$, $b = 904 \text{ \AA}^3$. Other color codes: C, grey; O, red; Cu (central), green; and Cu (upper and lower), blue. Hydrogen atoms are omitted for clarity. (c) Schematic view of the Cu_{24} cluster where blue and green spheres account for the twelve dimers per cluster.

water molecules: eight dimers have DMF molecules on both apical positions (16 DMF) and four dimers have 1:1 DMF: water (4 DMF and 4 water) (Table 2). That is, there are 20 coordinated DMF molecules per cluster and 4 water molecules. Taking the centre of the cluster as a reference, the dimers are located in a radial fashion; one of the apical ligands points to the internal cavity, while the other points to the exterior.

According to the chemical formula and including the removed 520 e^- with the SQUEEZE program (as explained in the single-crystal X-ray diffraction section), 24 DMF and 40 water molecules have been identified as crystallization molecules. As mentioned before, one of those internal water molecules is localized at the centre of the cluster, being the reference point around which the CCP disposition of the dimers produces the cluster.

The average diameters of the cluster are 32 \AA (including terminal ligands) and 24 \AA (excluding terminal ligands). Calculation of the diameter of the internal cavity omitting the guest molecules produces a value of 16 \AA (volume of 2145 \AA^3). Nevertheless, as observed in Fig. 2, if considering internal guest molecules, this cavity is quite smaller (904 \AA^3). In fact, the real value is slightly lower because, even if most of the ignored solvent molecules during structure refinement are located outside the internal cavities, some of them do correspond to the internal cavity.

The clusters are 3D packed as shown in Fig. 3. As observed, the central planes of the clusters (in green) are packed along the $[100]$ direction. The intercluster connections take place through hydrogen bonds between the coordinated DMF and H_2O molecules in the dimers and the guest molecules. Most of the extended analysis of the supramolecular

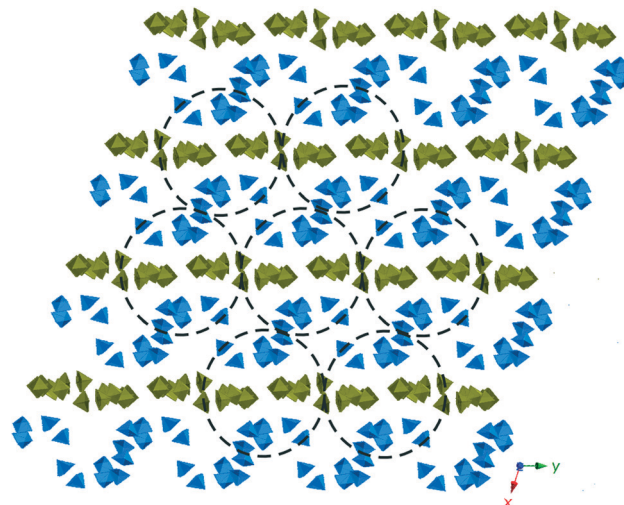


Fig. 3 $[001]$ view of the supramolecular 3D framework for compound 1. Each dotted circle marks a cluster. Green and blue polyhedra are the twelve dimers per Cu_{24} cluster. Solvent molecules and hydrogen atoms are omitted for clarity.

structure will be done in the section devoted to the comparison of 1 to the remaining similar clusters.

Infrared spectroscopy

IR data show characteristic bands for *m*-BDC ligands of compound 1 (Fig. 4). The bands at about 3402 cm^{-1} and $765\text{--}700 \text{ cm}^{-1}$ were assigned to the C–H bond of the benzene rings. The bands at 2930 cm^{-1} and 1680 cm^{-1} were assigned to the O–H and C=O bonds of the carboxylic groups, respectively. Finally, the bands at $1630\text{--}1441 \text{ cm}^{-1}$ were assigned to C=C stretching mode vibration.

Thermogravimetry

The thermogravimetric decomposition curve for compound 1 shows a two-stage mass loss (Fig. 5). The first step occurs between 20 and $230 \text{ }^\circ\text{C}$ with 27.2% weight loss. This value has been attributed to crystallization and coordination

Table 2 DMF and water molecules coordinated to Cu^{II} dimers

	DMF	DMF:H ₂ O (1:1)	H ₂ O
Number of Cu^{II} dimers	8	4	—
Number of molecules	16	4:4	—

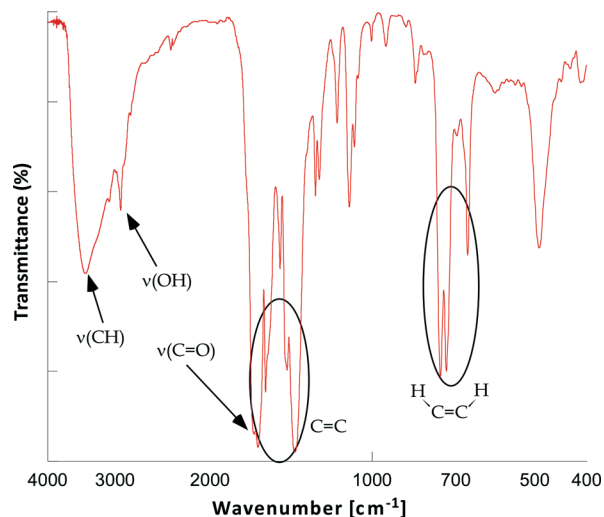


Fig. 4 Infrared spectra of compound 1.

molecules of water and DMF (25.9%). The second step is an overlapped process that occurs between 230 and 310 °C with 47.8% weight loss relative to the organic ligands of the cuboctahedron (41.8%) and coordinated DMF and water molecules (12.11%). The residue has been identified by X-ray powder diffraction as CuO [S.G. $C2/c$, $a = 46\,850\text{ Å}$; $b = 34\,230\text{ Å}$; $c = 51\,320\text{ Å}$; $\beta = 99, 52^\circ$].³¹

X-ray thermogravimetry

The thermal behaviour of compound 1 was also studied by X-ray thermogravimetry (Fig. S2, ESI†). Compound 1 maintains its crystallinity until 165 °C. At higher temperatures, the removal of DMF and H₂O solvent molecules

provokes the formation of an amorphous phase, forming CuO from 280 °C.

Comparison of similar Cu₂₄ clusters

A search in the CSD³² (Cambridge Structural Database) shows 594 structures with pentacoordinated copper dimers similar to the one exhibited by compound 1. However, just 7 of them are cuboctahedral Cu₂₄(*m*-BDC) clusters. Therefore, the crystal structures of these compounds have been analyzed. Their chemical formulae are [Cu₂₄(*m*-BDC)₂₄·(MeOH)₂₄]·xS¹⁸ (hexagonal) (2), *α*-MOP-1¹⁶ [Cu₂₄(*m*-BDC)₂₄·(DMF)₁₄(H₂O)₁₀]·50H₂O·6DMF·6C₂H₅OH (3), [Cu₂₄(*m*-BDC)₂₄·(S)₂₄]·xS¹⁷ (4), [Cu₂₄(*m*-BDC)₂₄(Py)₁₂(MeOH)₁₂]·xS¹⁸ (5), *c*-MOP-1¹⁶ [Cu₂₄(*m*-BDC)₂₄(H₂O)₂₄]·42H₂O (6), [Cu₂₄(*m*-BDC)₂₄(MeOH)₂₄]·xS¹⁸ (cubic) (7) and [Cu₂₄(*m*-BDC)₂₄(MeOH)₂₄]·xS¹⁸ (monoclinic) (8). Therefore, a similar arrangement is produced with other solvents distinct from DMF and water that act both as coordinated ligands and as crystallization molecules. In addition, the number of solvent molecules acting as crystallization molecules is variable.

Table S1 in the ESI† summarizes the most significant crystallographic parameters for those compounds. As previously mentioned, these 7 compounds have been selected because they exhibit similar Cu₂₄ clusters. However, their different packing fashions are reflected in the distinct cell parameters, and they are related to the variety of solvent molecules.

As previously mentioned, even if provided with the best possible structure refinement, we have not been able to localize all the crystallization molecules. In fact, a comparison of the *R* indices for the remaining similar compounds (Table S1, ESI†) indicates that in most of the cases structural refinement has been carried out by omitting the solvent molecules. However, those solvent molecules are responsible for the stabilization of the crystal structure. In fact, removal of DMF and H₂O molecules results in the collapse of the crystal structure as shown by thermogravimetric and thermogravimetry analyses (Fig. 5 and S2, ESI†).

If we analyze the packing of compound 1 (Fig. 3), we can observe the layered nature of the 3D framework. Thus, as previously mentioned, the central planes of the cluster (green) are packed along the [100] direction. This way, the dimers above and below these planes (blue) are localized in between. As observed in Fig. 6, layered frameworks can also be observed for compounds 2–5.

It is worth noting that compounds 3–5 are triclinic, and the clusters also exhibit the CCP fashion observed for 1. However, the cluster of compound 2 is of the HCP-type. Thus, this allows the unit cell to conserve the hexagonal symmetry (the space group for 2 is $P6_3/m$).

Compounds 6–8 also exhibit a CCP-type cluster, but they merit special attention. As observed in Table S1 (ESI†), structural parameters for cubic compounds 6 and 7 (the space group is $Im\bar{3}m$) indicate that they have the same skeleton, so they will be described together. Thus, as a result of the cubic space group, the 3D framework for compound 6 (and 7) is a

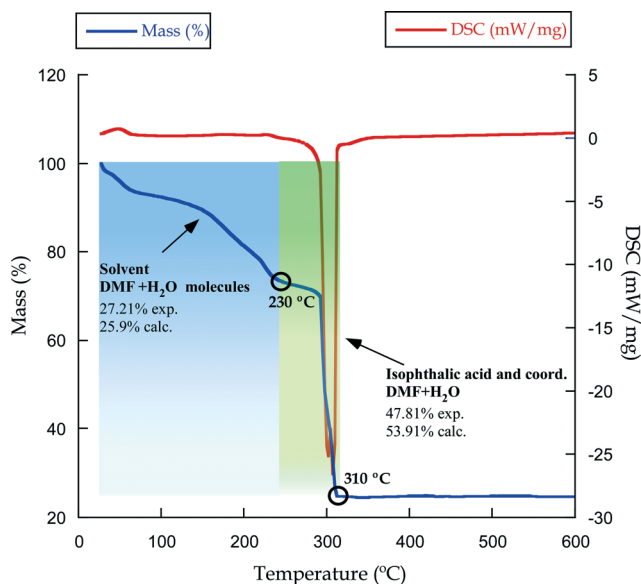


Fig. 5 Thermogravimetric analysis for compound 1.

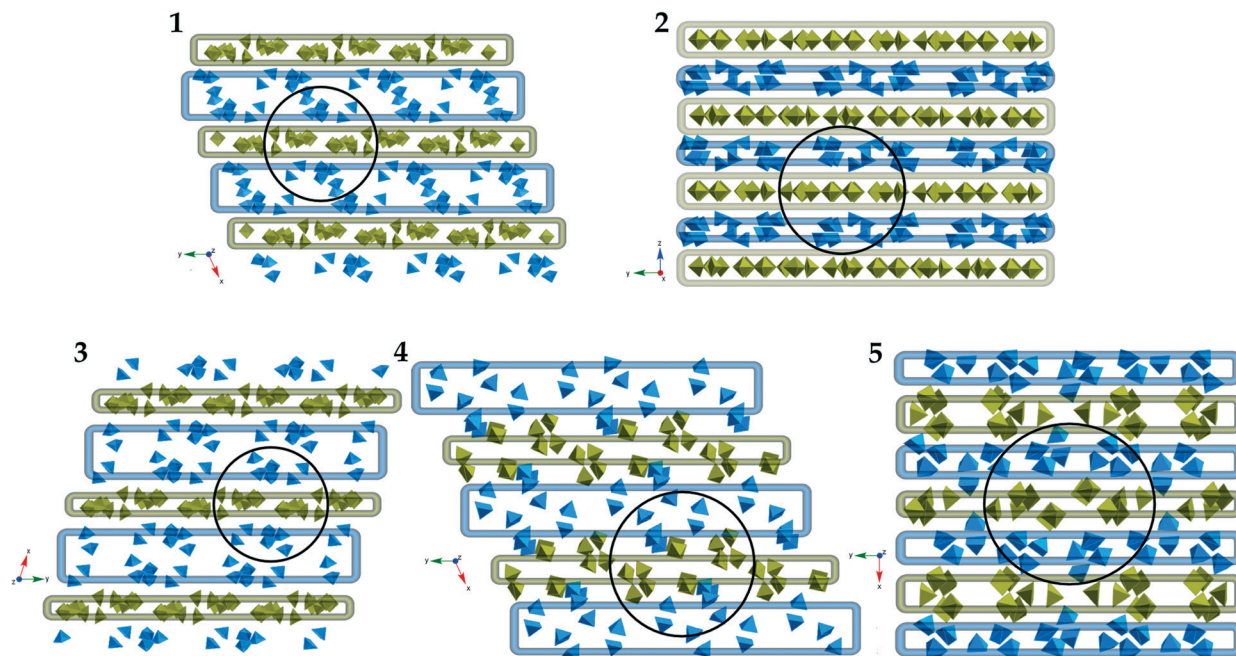


Fig. 6 Layered 3D frameworks for compounds 1–5. Dotted circles mark the Cu_{24} clusters. Green and blue polyhedra are the twelve dimers per Cu_{24} cluster.

layered structure (Fig. 7) where planes contain both types of dimers (blue and green ones). On the other hand, compound 8 adopts an intermediate packing fashion between the high symmetrical compound 6 (and 7) and the low symmetrical, triclinic compounds 1, 3, 4, and 5. In fact, two interpenetrated layered frameworks are observed for 8 (Fig. 7) where clusters are packed in perpendicular planes.

Therefore, the presence of MeOH in compounds 2 and 6 as a solvent gives rise to the highest symmetry, also producing both possible alternatives: hexagonal and cubic. These

ideal packing fashions can be observed in Fig. 8 where a different view of the 3D frameworks for compounds 2 (hexagonal) and 6 (cubic) is shown.

As mentioned before, we have made a special effort on locating the maximum number of molecules of solvent in the structural refinement of compound 1. As a consequence, we have located a molecule of water right in the centre of the cluster. Therefore, those central water molecules seem to be the reference for the clusters to be formed and for the packing to be extended along the three directions of space. On

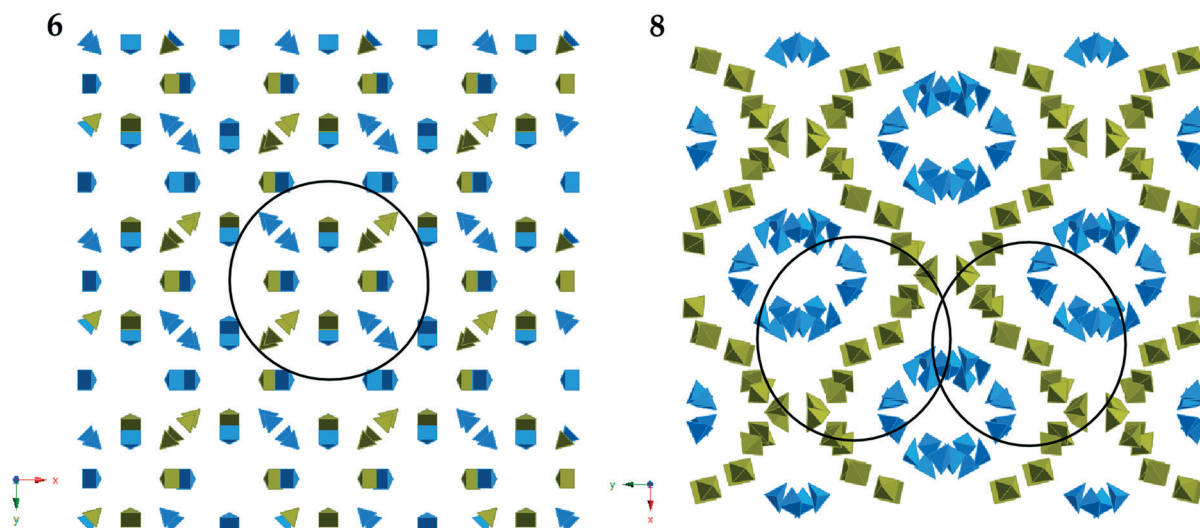


Fig. 7 3D frameworks for compounds 6 (or 7) and 8. Dotted circles mark the Cu_{24} clusters. Green and blue polyhedra are the twelve dimers per Cu_{24} cluster. Clusters for 8 are packed in two different orientations.

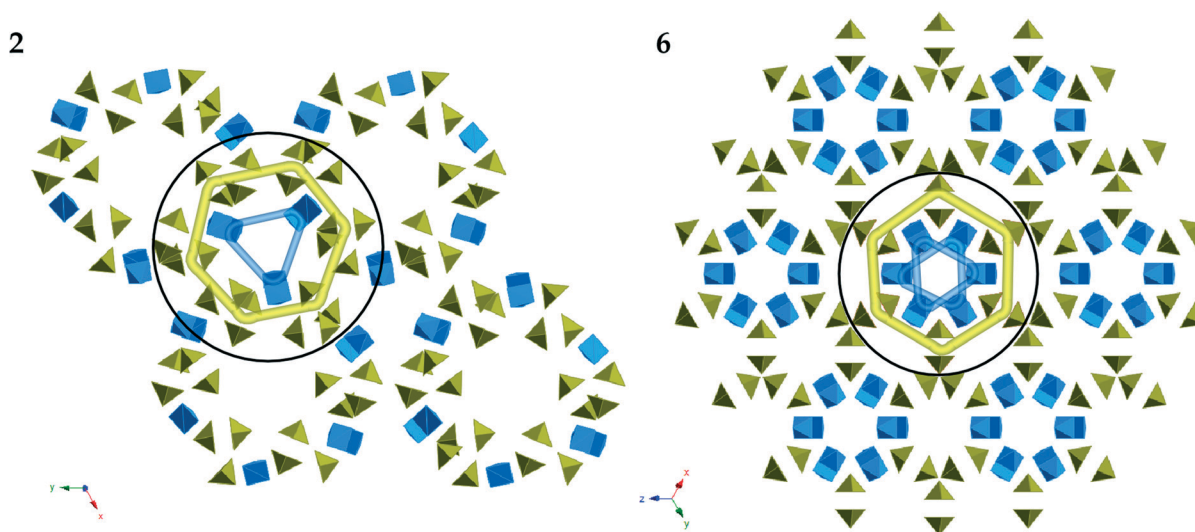


Fig. 8 Mother structures for Cu_{24} clusters: HCP-type (compound 2) and CCP-type (compounds 6 and 7).

the other hand, the fact that both possible clusters (cubic and hexagonal) are related to the close packing of spheres makes us think of the similarities between these 3D arrays and the simple metal frameworks. At this point of the discussion, it is worth noting that small molecules acting as coordinated ligands and as crystallization molecules are able to accumulate quite a high number of metal ions producing a variety of solids that are similar but not equal. So, we wonder if geological accumulation of metal deposits might have something to do with the formation of clusters like compounds 1–8.

Conclusions

A comparison of compound 1 with similar ones found in the literature reveals the existence of two mother structures related to the hexagonal and cubic close packing of polyhedra. Derivatives of these mother compounds depend on the solvents used in the syntheses. Solvent molecules act both as ligands and as crystallization guest molecules. The variety in 3D frameworks observed for the eight compared compounds is attributable to the fact that solvents of a different nature can play the same roles. Thus, not only the nature but also the number of solvent molecules is a variable for the analyzed compounds, accounting for the flexibility of these host networks to accommodate different guests.

Acknowledgements

This work was supported by the “Ministerio de Economía y Competitividad” (MAT2013-42092-R), the “Gobierno Vasco” (Basque University System Research Groups, IT-630-13) and UPV/EHU (UFI11/15). The technical and human support provided by SGIker is gratefully acknowledged. E. Amayuelas and A. Fidalgo-Marijuan thank the UPV/EHU formation scholarships.

Notes and references

- 1 H. Furukawa, J. Kim, N. W. Ockwig, M. O’Keeffe and O. M. Yaghi, *J. Am. Chem. Soc.*, 2008, **130**, 11650–11661.
- 2 Y. Ke, D. J. Collins and H.-C. Zhou, *Inorg. Chem.*, 2005, **44**, 4154–4156.
- 3 G. J. McManus, Z. Wang and M. J. Zaworotko, *Cryst. Growth Des.*, 2004, **4**, 11–13.
- 4 T.-F. Liu, Y.-P. Chen, A. A. Yakovenko and H.-C. Zhou, *J. Am. Chem. Soc.*, 2012, **134**, 17358–17361.
- 5 M. Tonigold, J. Hitzbleck, S. Bahnmueller, G. Langstein and D. Volkmer, *Dalton Trans.*, 2009, 1363–1371.
- 6 X. Li, R. Cao, D. Sun, W. Bi, Y. Wang, X. Li and M. Hong, *Cryst. Growth Des.*, 2004, **4**, 775–780.
- 7 L. Han, Y. Zhou, W.-N. Zhao, X. Li and Y.-X. Liang, *Cryst. Growth Des.*, 2009, **9**, 660–662.
- 8 R. Mondal, T. Basu, D. Sadhukhan, T. Chattopadhyay and M. K. Bhunia, *Cryst. Growth Des.*, 2009, **9**, 1095–1105.
- 9 B. Moulton and M. J. Zaworotko, *Chem. Rev.*, 2001, **101**, 1629–1658.
- 10 *Advanced Topics on Crystal Growth*, ed. S. O. Ferreira, 2013.
- 11 H. Furukawa, K. E. Cordova, M. O’Keeffe and O. M. Yaghi, *Science*, 2013, **341**, 974.
- 12 M. O’Keeffe and O. M. Yaghi, *Chem. Rev.*, 2012, **112**, 675–702.
- 13 M. Li, D. Li, M. O’Keeffe and O. M. Yaghi, *Chem. Rev.*, 2014, **114**, 1343–1370.
- 14 T. R. Cook, Y.-R. Zheng and P. J. Stang, *Chem. Rev.*, 2013, **113**, 734–777.
- 15 F. Gandara, H. Furukawa, S. Lee and M. Yaghi Omar, *J. Am. Chem. Soc.*, 2014, **136**, 5271–5274.
- 16 M. Eddaoudi, J. Kim, J. B. Wachter, H. K. Chae, M. O’Keeffe and O. M. Yaghi, *J. Am. Chem. Soc.*, 2001, **123**, 4368–4369.
- 17 J.-R. Li and H.-C. Zhou, *Nat. Chem.*, 2010, **2**, 893–898.
- 18 B. Moulton, J. Lu, A. Mondal and M. J. Zaworotko, *Chem. Commun.*, 2001, 863–864.

- 19 I. Bruzaite, V. Snitka, V. Mizariene, L. Limanauskas and V. Lendraitis, *Int. J. Nanomanuf.*, 2010, 5, 205–213.
- 20 W. Yinghua, *J. Appl. Crystallogr.*, 1987, 20, 258–259.
- 21 *CrysAlisPro Software System*, Agilent Technologies UK Ltd., Oxford, UK, 2012.
- 22 L. Palatinus and G. Chapuis, *J. Appl. Crystallogr.*, 2007, 40, 786–790.
- 23 G. M. Sheldrick, *Acta Crystallogr., Sect. A: Found. Crystallogr.*, 2008, 64, 112–122.
- 24 O. V. Dolomanov, L. J. Bourhis, R. J. Gildea, J. A. K. Howard and H. Puschmann, *J. Appl. Crystallogr.*, 2009, 42, 339–341.
- 25 P. Roman and J. M. Gutierrez-Zorrilla, *J. Chem. Educ.*, 1985, 62, 167–168.
- 26 A. L. Spek, *Acta Crystallogr., Sect. C: Struct. Chem.*, 2015, 71, 9–18.
- 27 A. Fidalgo-Marijuan, G. Barandika, B. Bazan, M. K. Urtiaga and M. I. Arriortua, *Polyhedron*, 2011, 30, 2711–2716.
- 28 A. Fidalgo-Marijuan, G. Barandika, B. Bazan, M. K. Urtiaga and M. I. Arriortua, *CrystEngComm*, 2013, 15, 4181–4188.
- 29 A. Fidalgo-Marijuan, G. Barandika, B. Bazan, M. K. Urtiaga, L. Lezama and M. I. Arriortua, *Inorg. Chem.*, 2013, 52, 8074–8081.
- 30 A. Fidalgo-Marijuan, G. Barandika, B. Bazan, M. K. Urtiaga, E. S. Larrea, M. Iglesias, L. Lezama and M. I. Arriortua, *Dalton Trans.*, 2015, 44, 213–222.
- 31 S. Asbrink and L. J. Norrby, *Acta Crystallogr., Sect. B: Struct. Sci., Cryst. Eng. Mater.*, 1970, 26, 8–15.
- 32 F. H. Allen, *Acta Crystallogr., Sect. B: Struct. Sci.*, 2002, 58, 380–388.